J. Fluid Mech. (1992), *vol.* 244, *pp.* 225–240

Shock-induced collapse of single cavities in liquids

By N. K. BOURNE AND J. E. FIELD
Cavendish Laboratory, Madingley Road, Cambridge, CB3 0HE, UK

(Received 11 December 1991 and in revised form 13 April 1992)

A two-dimensional method was used to observe the interactions of plane shock waves with single cavities. This allowed study of processes occurring within the cavity during collapse. Results were obtained from high-speed framing photography. A variety of collapse shock pressures were launched into thin liquid sheets either by firing a rectangular projectile or by using an explosive plane-wave generator. The range of these shock pressures was from 0.3 to 3.5 GPa. Cavities were found to collapse asymmetrically to produce a high-speed liquid jet which was of approximately constant velocity at low shock pressures. At high pressures, the jet was found to accelerate and crossed the cavity faster than the collapse-shock traversed the same distance in the liquid. In the final moments of collapse, high temperatures were concentrated in two lobes of trapped gas and light emission was observed from these regions. Other cavity shapes were studied and in the case of cavities with flat rear walls, multiple jets were observed to form during the collapse.

1. Introduction

The features of cavity collapse explored in this paper have importance in several diverse areas of fluid mechanics. Cavitation erosion has merited much recent attention (Lauterborn & Bolle 1975; Tomita, Shima & Ohno 1984, Tomita & Shima 1986; Grant & Lush 1987; Vogel, Lauterborn & Timm 1989) but was discussed as early as the 1890s by the British Admiralty (Parsons & Cook 1919) and first investigated systematically by Cook (1928) who attributed observed surface pitting to 'erosion by water hammer'. Bowden & Yoffe (1952) were amongst the first workers to highlight the role of cavity collapse in the initiation of explosives. Pores exist in pressed compacts and cavitated liquids and also, as a result of cooling stresses, in cast crystalline energetic materials. Shocks running into such materials trigger pore collapse which initiates fast reaction in the vicinity of the void (Coley & Field 1973; Taylor 1985; Johnson 1987). Initiation of reaction has been attributed to high temperatures produced by either adiabatic compression of trapped gases (Chaudhri & Field 1974; Starkenberg 1981), viscous flow of the matrix material during pore collapse or hydrodynamic heating produced in the course of asymmetric closure (Mader 1964; Mader & Kershner 1985; Frey 1985; Bourne & Field 1989, 1991). Pore space has proved so successful in providing potential reaction sites that glass microballoons are added to commercial blasting explosives in order to improve their sensitivity to shock (see, for example, Leiper, Kirby & Hackett 1985).

Amongst the earliest mathematical descriptions of the collapse of a spherical bubble was that due to Besant (1859). Lord Rayleigh (1917) produced a comprehensive analysis of a vapour-filled spherical cavity collapsing in an infinite, inviscid, incompressible fluid at constant ambient pressure. Refinements to the Rayleigh approach have subsequently added the real-fluid effects of temperature,

liquid compressibility, viscosity and surface tension. A widely used solution taking into account the above and adding liquid compressibility was produced by Gilmore (1952). Kornfeld & Suvorov (1944) were amongst the first to suggest that cavities might collapse asymmetrically to produce a liquid jet, whilst Walters & Davidson (1962, 1963) presented theoretical and experimental results in which a 'tongue of liquid' was found to be projected into bubbles accelerated by a gravitational field. Benjamin & Ellis (1966) observed the formation of a liquid microjet in their classic photographic study and provided a theoretical discussion of the asymmetric collapse.

The asymmetry of the collapse is a result of a pressure gradient across the bubble. In the case where this gradient is provided by a solid boundary, a jet forms which is directed onto the surface (Plesset & Chapman 1971). The situations considered above may be classified as steady-state collapses under temporally static pressure fields. This may be contrasted with the collapses experienced by a cavity when a transient pressure pulse such as a shock wave passes over it. In this case a microjet forms generally travelling in a direction perpendicular to the shock front (Dear & Field 1988*a*; Bourne 1989).

This paper aims to examine jet formation in single cavities as a function of several parameters. Cavity geometry is varied to include circular, elliptical, rectangular and triangular voids. Secondly, collapse-shock pressure is adjusted to observe effects upon jet velocities and the hydrodynamics of jet formation at high shock pressures. Finally, cavity size is examined as a function of jet velocity.

2. Experimental

A method in which liquid-drop impact phenomena might be studied two-dimensionally was suggested by Brunton (1967). He thought that discs might be used to replace drops in rain erosion experiments and, with Camus, designed an apparatus in which a disc of water was held under its own surface tension between two glass blocks and impacted with a metal slider (Brunton & Camus 1970; Camus 1971). The technique was adapted by Dear (1985) to use water with 12% by weight gelatine to give more accurate control over the geometry of the liquid impacted (Dear & Field 1988*a*; Field, Lesser & Dear 1985). Dear employed the method to look at a few simple cavity collapse configurations (Dear 1985; Dear & Field 1988*b*).

The advantage of studying bubble collapse two-dimensionally is that details of processes occurring within the bubble can be followed without the refraction problems associated with viewing through a curved wall. The gel layer was cast in a mould from 12% by weight of gelatine in water at room temperature (to give a gel density, $\rho = 970 \pm 50$ kg m^{-3}). The mould faces were lightly greased and covered with a thin plastic film. The gelatine layers produced, with plastic sheets attached, could be kept for several days. Cavities of any shape or array geometry were then produced by punching out suitable shapes. When shocked the gelatine lost its viscoelastic properties, undergoing a phase change.

Both toughened-glass and polymethylmethacrylate (PMMA) blocks were used to confine the sample. The thickness of the blocks was designed to ensure that no rarefaction reached the shock running in the gelatine until it had passed the areas of interest, for example the cavities. The free surfaces of the gelatine sheet within the blocks were butted against PMMA spacers to prevent rarefactions relieving the shock pressure from the sides.

The range of shock pressures introduced varied from 0.3 GPa from a flier plate to 10 GPa from a detonator. Lower shock pressures were produced by firing a

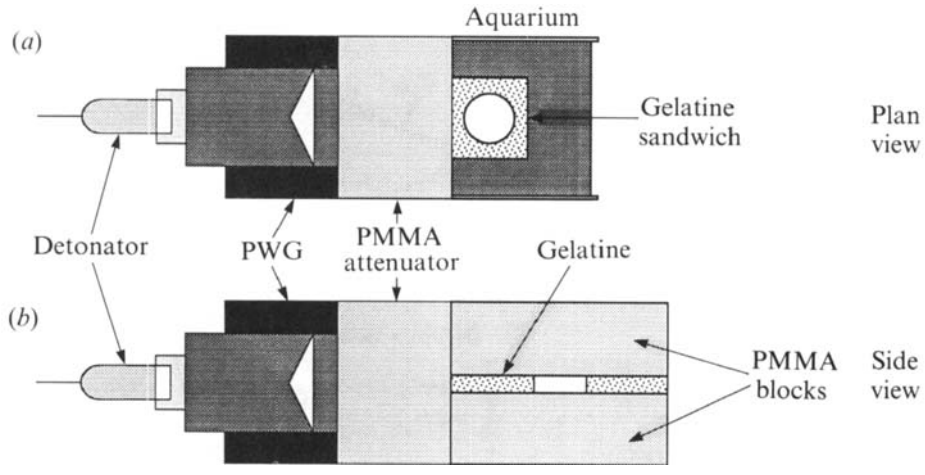

FIGURE 1. (*a*) PWG with an aquarium. The water impedance matches the fluid gelatine, avoiding the need for glass blocks which shatter, obscuring the experiment and destroying the confinement. (*b*) The PWG with transparent blocks cemented to the gap.

rectangular, phosphor–bronze flier plate between the transparent blocks so that it impacted the front surface of the gelatine. The slider had a circular section removed to reduce its mass. The velocity of the slider was about 150 m s^{-1} and it had a mass of 5.5 g. The slider was fired from a rectangular-bore gas gun (Hutchings, Rochester & Camus 1977).

To introduce shocks of 2 GPa or greater into a sample, a calibrated explosive plane-wave generator (PWG) was used (Leiper & Steele 1984), which consisted of an outer cylinder of a plastic explosive with a conical cavity removed into which a nitroglycerine/salt mixture was packed. The output shock pressure was controlled by the use of a variable PMMA attenuator to which prepared samples were bonded directly. The plane wave emerging from the attenuator blocks was 40×40 mm^2. The shock wave entered directly both the glass/PMMA blocks and the gelatine if attached to the face of the PWG (figure 1). This resulted in strong shocks in the containing blocks running ahead of those in the gelatine. These caused damage within the blocks and spurious interfacial effects which obscured detail in the gelatine. Some experiments were carried out in water-filled tanks (aquaria) in which the gelatine slab was sandwiched between two other gel slabs to isolate the gas-filled cavities. The base of the tank was the PMMA attenuator, whilst the sides were constructed from thin PMMA sheets. There was thus no impedance mismatch between the gel and its surroundings. The shock pressure in the water corresponding to the exit pressure from the PMMA gap was calculated from Hugoniot data (Walsh & Rice 1957; Marsh 1980; Mitchell & Nellis 1982).

The shock introduced by the flier plate was of magnitude 0.3 GPa and of negligible rise time. This pressure was maintained around the cavity until rarefactions reached the collapse site. It was found, by varying the block thickness, flier dimensions, and the size of the gelatine sheet, that rarefactions did not affect the jet velocity once the shock had passed and that the jet velocity remained constant even though the driving pressure was removed. In the case of the PWG, the shock front was again sharp and the peak pressure is quoted below. The pressure behind the shock front decays rapidly to the Chapman–Jouget pressure for the explosive but remains driven by the expanding product gases. Collapses are in all cases complete before rarefactions arrive at the cavity site to relieve pressures.

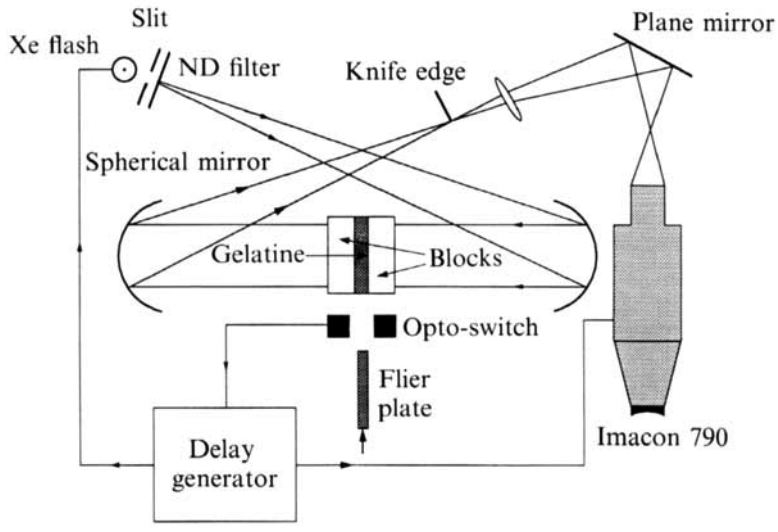

FIGURE 2. Experimental schlieren system employed in the work. The mirrors are of diameter 10.1 cm and of focal length 1.22 m.

The collapses were photographed using Hadland Imacon 790 and 792 cameras in framing and streak modes; the framing rates were varied from 2×10^5 to 5×10^6 frames per second. The sample was mounted in a conventional two-mirror schlieren system (figure 2). The flash source was a Xenon QCA5 tube which delivered a stored energy of 150 J in approximately 100 μs. The flash and camera were triggered via the three-channel delay generator by the flier-plate cutting an infra-red beam on exiting the gun barrel or by a photodiode picking up the detonation wave via an optical fibre buried in the PWG.

3. Results

3.1. *Circular cavities*

Figure 3 shows an Imacon 790 sequence composed from frames from separate experiments. A 12 mm, air-filled cavity collapses in gelatine after a shock of pressure 0.3 GPa runs over it. The times below each frame indicate that interval after frame (i) and the exposure time for each frame is about 0.5 μs. In frame (i) the collapse shock, labelled S, is visible halfway up the frame having entered from below. The shock is not well defined because the knife-edge is positioned in the spatial frequency corresponding to the cavity's gas content, which is in this case air. The gas appears dappled due to disturbance by the blast of air trapped ahead of the flier-plate and expelled from the gun barrel. The upstream cavity wall begins to spall across the cavity driving an air shock which appears as a white line, A, travelling at about 330 m s^{-1}. In frames (ii) and (iii), taken at 10 μs intervals, the air shock travels across the cavity and reflects at the downstream wall. The radius of curvature of the shock increases as it traverses the cavity. Frame (iv), taken 70 μs after frame (i), shows the cavity after the air shock has undergone its first reflection at the upstream wall. Between frames (iii) and (iv) the upstream wall has involuted to form a jet which subsequently crosses the cavity. The air shock has assumed a convoluted form and continues to bounce around in the contracting volume throughout the rest of the

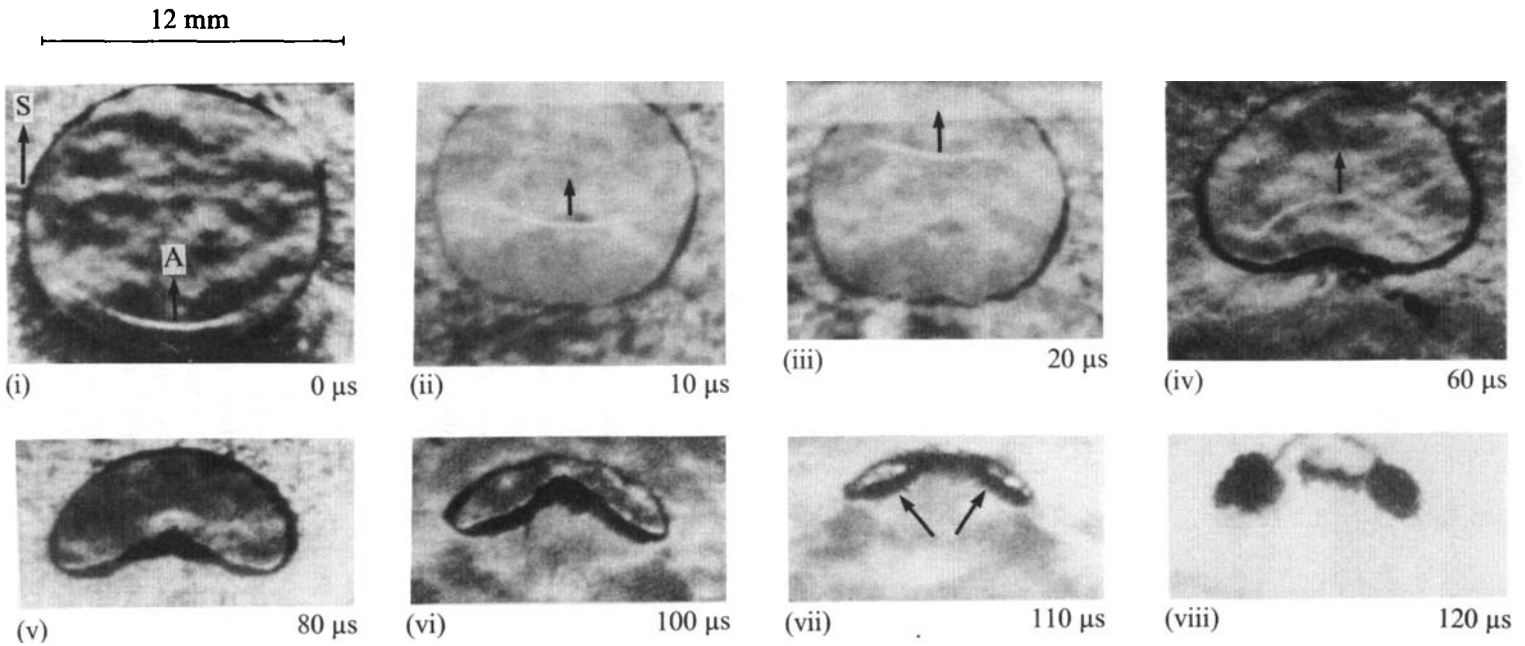

FIGURE 3. A 12 mm cavity in gelatine collapses after interaction with a 0.26 GPa shock. The exposure time for each frame is 0.5 μs. The time interval after frame (i) is quoted below each frame. Note the air shock, A, travelling across frames (i) to (iii). Also the jet formed by frame (iv) which hits the downstream cavity wall between frames (vi) and (vii). Penetration of the jet isolates two lobes of trapped gas, L, in frame (vii) whilst jet penetration forms a pair of linear vortices which travel downstream in the flow behind the shock.

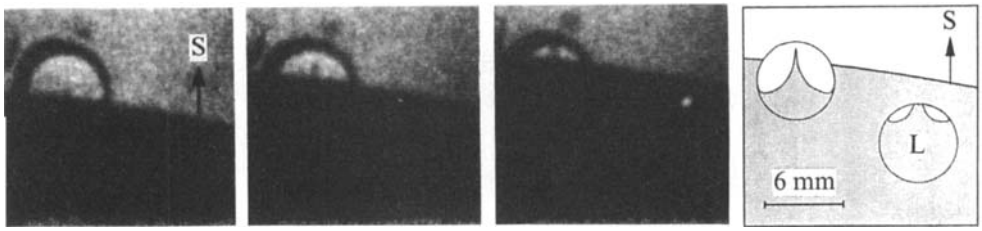

FIGURE 4. A high-speed jet travels across a 6 mm cavity under a 1.88 GPa shock from a PWG. A schematic of the collapse geometry is shown beside the sequence. The jet travels at about 5 km s^{-1}. Interframe time 0.4 μs.

sequence. Frames (v) and (vi) show the jet crossing the cavity. It hits the downstream wall between frames (vi) and (vii), and the impact sends a shock out into the surrounding liquid. In frame (vii) the jet begins to penetrate the interface isolating two lobes of trapped and highly compressed gas labelled L. Frame (viii) shows the final state of the collapsed cavity. Jet penetration has created a pair of linear vortices which subsequently travel downstream in the flow behind the shock. The time from the initial impingement of the shock on the upstream wall to the impact of the jet on the downstream wall (which we shall refer to as the *collapse time*, τ, throughout the rest of this paper) is about 115 μs.

Collapses at shock pressures up to 3.5 GPa have been studied and jet velocities and collapse times have been measured for 3, 6 and 12 mm diameter cavities. The mechanism of the collapse appears qualitatively to be the same at these elevated pressures as it was in the flier experiments. However it is possible to achieve extremely high jet velocities. Figure 4 shows two 6 mm cavities collapsing in an aquarium. The shock pressure is 1.9 GPa and the sequence was taken using an Imacon 790 and has an interframe time of 0.4 μs. The two cavities are inclined to one another as shown in the schematic displayed with the sequence. Details of processes occurring behind the incident shock are obscured by its curvature. However, a high-speed jet can be seen travelling across the cavity ahead of the incident shock. The jet is travelling at 5 km s^{-1}. The calculated water hammer pressure at jet impact at the downstream wall is 7.5 GPa for this jet. The jet velocity is 7.5 times the particle velocity in the medium. The bright flashes (L) seen in frame (iii) are light emitted by a hidden cavity in the final stages of collapse. This luminescence is believed to result from free-radical creation and radiative recombination (Dear, Field & Walton 1988) in the high-temperature gas trapped within the cavity. This phenomenon is explored in more detail in a later sequence.

It is clear from the sequence of figure 4 that jet impact has occurred in this case at the downstream cavity wall before the incident shock has arrived at the same position. This results in a situation where the shock resulting from the jet impact travels ahead of the collapsing shock. Chaudhri, Almgren & Persson (1982) have observed analogous behaviour in the three-dimensional collapse of a hollow aluminium sphere by a shock from a PETN charge. Clearly the hydrodynamics of jet formation at high pressures can result in much higher jet velocities than those expected from an acoustic approximation where the jet velocity would be, conserving momentum, twice the particle velocity behind the collapse-shock.

Typical cavity collapses at shock pressures P have been presented above. A parameter characterizing a collapse is the collapse time τ, defined to be the time from

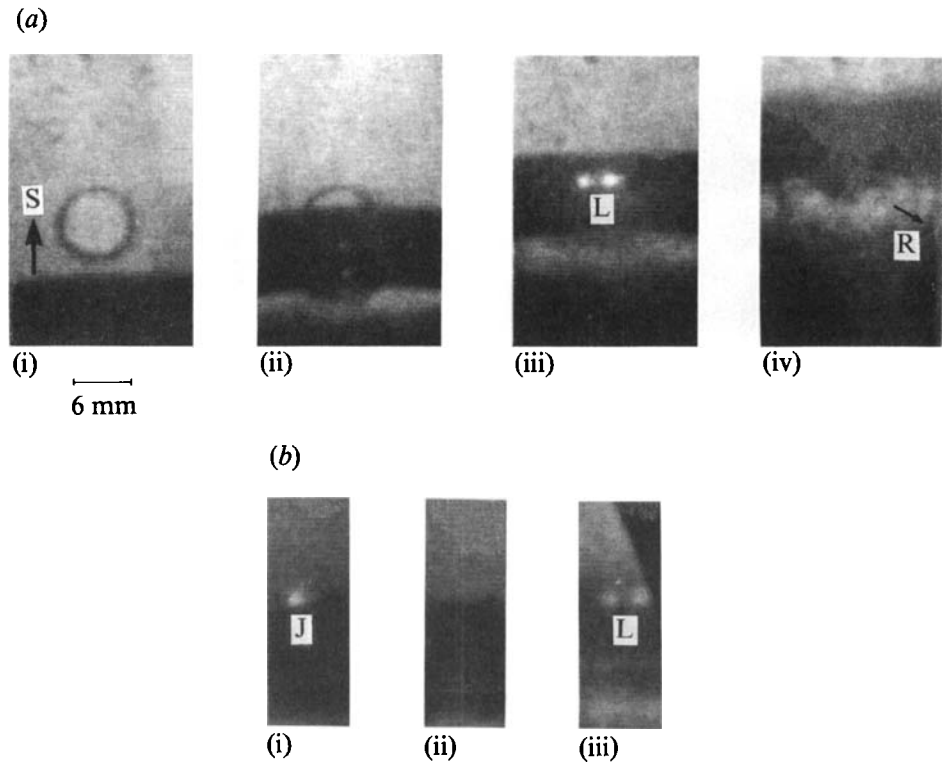

FIGURE 5. A 1.9 GPa shock wave interacts with a 6 mm cavity. Luminescence, L, is observed to occur in frame (iii) of (*a*). The interframe time is for (*a*) 2 μs. The luminescence event is seen in more detail in (*b*) and is observed to consist of two events J and L. The sequence is taken with an Imacon 790 and utilizes schlieren photography. Interframe time 0.2 μs.

the incident shock hitting the upstream wall to the time at which the liquid jet hits the downstream wall. This definition differs from that used for spherical collapses, which is the time from maximum to minimum volume (and of course is smaller). Table 1 shows measured jet velocities and collapse times from this work for cavities of varying diameters placed in differing geometries. Jet velocities and collapse times are quoted for the shocks of 0.3, 0.5, 1.9 and 3.5 GPa. Particle velocity behind the shock is calculated from the Hugoniot relation for water since the shock pressure is known.

A sequence is shown in figure 5 in which a 6 mm cavity collapses in gelatine. The shock is of pressure 1.9 GPa and is introduced with a PWG. The experiment is carried out in a water-filled aquarium. The gelatine sheet with punched bubble is sandwiched between two further gelatine sheets isolating a disk-shaped cavity of depth 3 mm and diameter 6 mm. The shock is not completely planar as it exits the PMMA gap and so the collapse is observed from the side through a curved shock front. This distorts certain details of the collapse because of refraction. Four frames from the original sequence are reproduced in figure 5(*a*). The interframe time is 2 μs. In frame (i) the bubble can be seen with the shock, S, entering from below. In frame (ii) the shock has travelled across about half of the cavity and the collapse has started. In frame (iii) the shock has obscured the entire area of the cavity. Spalled PMMA travelling behind the shock front obscures the lower part of the frame. Two bright areas, L, of emitted light are visible. By frame (iv) the collapse is complete and a rebound shock, R, is

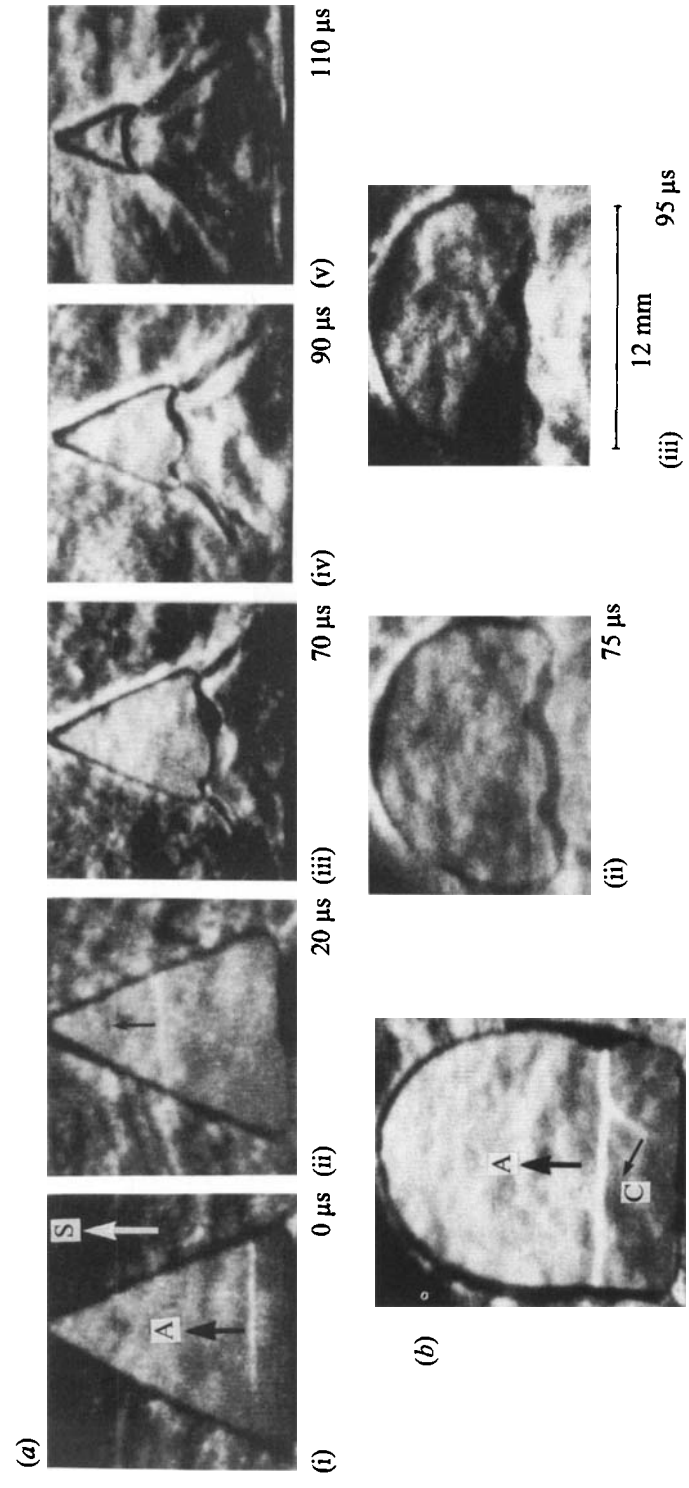

FIGURE 6. Flat-walled geometries collapsing when a 0.3 GPa shock passes over them. In (*a*) a triangular and in (*b*) a semicircular cavity collapses. Note the creation and movement of jets on the upstream wall. Also the air shocks A, and the corner wave C.

visible moving into the fluid centred on the jet-impact site. The collapse time of the cavity is approximately 5 μs giving a jet velocity of about 1.2 mm μs^{-1}. Luminescence was also observed from 3 and 12 mm cavities collapsed under the same shock regimes. When the shock pressure was reduced to 0.5 GPa, no luminescence was observed. The two flashes originate from the two isolated lobes of gas seen in figure (iii) and correlate in position with these.

The same experiment was repeated at a higher framing rate and the results are presented in figure 5(*b*). The framing rate has now been increased so that the interframe time is 0.2 μs and the exposure time is 40 ns. In frame (i) a single flash of light, J, is observed which has died out by frame (ii). In frame (iii) two patches of light, L, are seen which appear less bright than J. The luminescence at the points J and L is thought to be associated with the impact of jet (J) and the compression of gas in the lobes (L). The dark areas on the right-hand side of frames (ii) and (iii) are blanking marks introduced by the Imacon's display circuitry.

3.2. *Other single-cavity geometries*

Several other cavity geometries have been collapsed with 0.3 GPa shocks in order to observe the formation of jet structures on the upstream cavity wall. The shapes include square, semicircular, triangular and elliptical cavities. The behaviour can be classified according to the geometry of the upstream cavity wall. In the case of flat upstream walls, several jets are formed which migrate along the surface. When a triangular cavity is orientated so that the shock initially encounters the apex of the cavity, the jet is formed by a 'shaped-charge' mechanism (see for example, Birkhoff *et al.* 1948). With an elliptical wall it is possible to so orient the cavity that the plane shock meets a wall which sweeps to right and left of the point of impact with a differing radius of curvature.

Figure 6 shows the collapse of two flat-walled geometries when hit by a 0.3 GPa shock. In (*a*) the cavity is triangular and the rear wall is 5 mm in length. The incident shock, S, and the air shock, A, can be seen in frame (i). In frame (ii) the air shock has traversed a portion of the cavity whilst deformation of the corners has begun. By frame (iii), which was taken 70 μs after frame (i), the upstream wall has developed two small jets which migrate along the wall towards one another at a characteristic velocity of 33 ± 1 m s^{-1}. In frame (v), taken 110 μs after frame (i), the jets coalesce into a single entity which crosses the cavity to impact the cavity apex.

Figure 6(*b*) shows an analogous geometry in which a 0.3 GPa shock collapses a semicircular cavity whose upstream wall is of length 12 mm. In frame (i) the air shock, A, and the corner waves, C, propagate within the cavity as the upstream wall deforms. In frame (ii), taken 75 μs after frame (i), small jets can be seen migrating towards one another along the upstream wall at a velocity of 46 ± 2 m s^{-1}. They coalesce in frame (iii).

A similar jet-migration velocity was measured when a square cavity was collapsed. The sequence is not reproduced here since the behaviour is qualitatively the same as that in figure 6(*b*). In all cases the observed jet migration velocities were constant throughout the collapse and the jets originated from the corners of the cavities. The angle made by the upstream wall with the two side walls controlled the migration velocity.

Figure 7 shows the collapse of an elliptical cavity with its major axis angled at 55° to the perpendicular to the shock front. Again the shock pressure is 0.3 GPa and the shock is introduced by flier-plate impact. The three frames presented show the development of a jet travelling perpendicular to the shock front. It may be expected

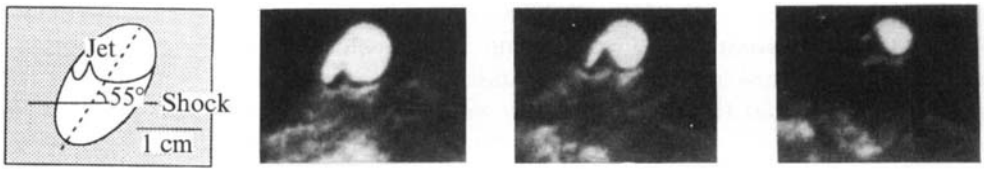

FIGURE 7. Elliptical cavity collapsing in gelatine. The cavity is inclined at 55° to the incident shock as shown in the schematic. The jet travels perpendicular to the shock front. Interfame time 10 μs.

that the difference in curvature either side of the point of impact may result in the jet deviating to travel along the major axis of the cavity. This is not observed in the figure. In other work when a detonator was used to provide a higher shock pressure, a sequence in which the jet did appear to deviate towards the major axis was obtained.

4. Discussion

4.1. *Circular cavities*

The sequence of figure 3 can be used to extract distance-time information for the wall and wave motions along an axis through the centre of the cavity. An x-t representation of the collapse is shown in figure 8 with the experimental points derived from measurements taken from the sequence along the dashed axis indicated in the schematic. The figure thus represents a streak reconstruction of the collapse. The following features can be seen. The jet formed by involution of the upstream wall travels at a constant velocity of 100 m s^{-1} across the cavity once an impulse has been given to the wall by the incident shock. Meanwhile, the downstream cavity wall remains rigidly fixed throughout the collapse until hit by the jet. The air shock can be seen bouncing within the cavity at close to its acoustic velocity. Note that here the jet velocity is an order of magnitude less than the incident shock velocity.

When smaller cavities are used the collapse behaviour is qualitatively identical with that shown in figure 3. However, jet velocities are elevated as cavity diameters are reduced given that a particular incident shock pressure is held constant. The jet velocity for a 3 mm cavity for instance is 300 m s^{-1}. This is close to twice the particle velocity which represents the expected value for a spalled one-dimensional plug of liquid in an acoustic approximation.

The data of table 1 show that increasing shock pressure increases jet velocities as expected. Additionally it is clear that jet velocity is highest for the cavities with the smallest radius of curvature at any particular incident pressure (see for example the data for 1.9 GPa). In figure 9, jet velocities are shown plotted against incident shock pressure for 6 mm diameter cavities collapsed in gelatine by shocks of pressure 0.3 to 3.5 GPa. The velocities are calculated by measuring the collapse time from framing sequences, which limits the resolution of the measurement to the inter-frame time of the camera used. For the strongest shocks, cavities are collapsed in a few microseconds and so sequences comprising only one or two frames give large errors in the plotted velocities. However, such error bars may be regarded as pessimistic since the jet is known to be travelling at approximately constant velocity and the error in distance measurement is small.

The Hugoniot for water, based on data from Marsh (1980), divides the graph into two regions. The region below the Hugoniot represents states for which the jet

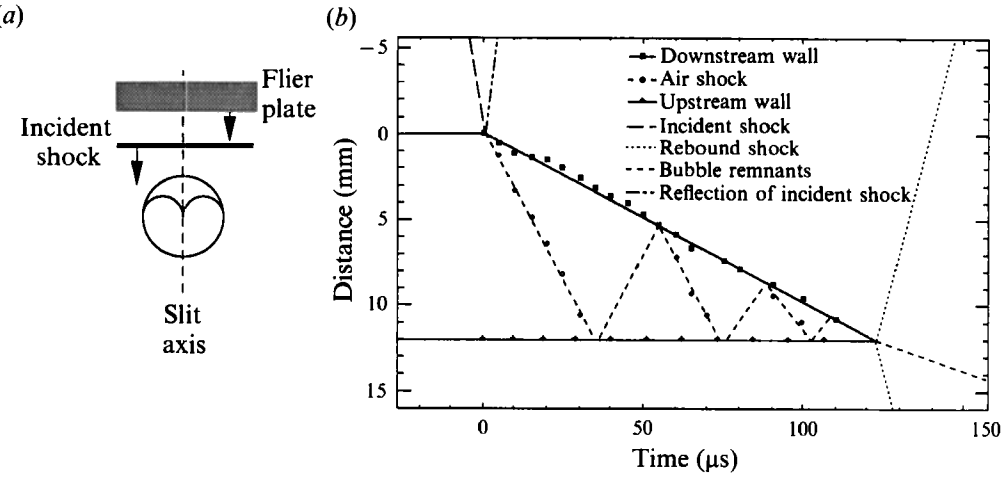

FIGURE 8. Data for the collapse of a 12 mm cavity taken along a line through the centre of the cavity and perpendicular to the shock front shown in (*a*). In (*b*) each wall and wave motion is represented. Note the constant velocity of the jet and the fixed downstream cavity wall. Data are derived from measurements taken from figure 3.

Shock pressure P (GPa)	Particle velocity (m s^{-1})	Cavity diameter (mm)	Geometry	Jet velocity (m s^{-1})	Collapse time (μs)
0.3	150	3A	Cavity and particle side by side	187±5	15±1
0.3	150	3B	Cavity before particle on axis	300±5	10±1
0.3	150	3C	Particle before cavity on axis	150±5	20±1
0.5	250	3	Single cavity in gelatine	3200±600	1.0±0.2
1.9	680	3	Single cavity in gelatine	4000±2000	1.0±0.5
0.3	150	6	Single cavity in gelatine	147±5	40±1
0.5	250	6	Single cavity in gelatine	1500±400	5±1
1.9	680	6	Single cavity in gelatine	3300±300	1.8±0.2
3.5	1030	6	Single cavity in gelatine	8000±4000	1±0.5
0.3	150	12	Single cavity in gelatine	130±5	100±5
1.9	680	12	Single cavity in gelatine	1500±200	8±1

TABLE 1. Data summarizing single-cavity collapse parameters at various incident shock pressures: A, B, C refer to the geometries in which cavities were placed close to lead particles in differing orientations with respect to the incident shock. The error in the collapse time is derived from the framing rate at which particular sequences were taken.

velocity is less than the shock velocity and that above represents jet velocities which are in excess of the shock velocity. Clearly it is possible for the jet velocity to rise to several times that of the shock velocity in the matrix. This means that signals can be propagated ahead of the shock front from the point of jet impact in an inert material or that initiation can be induced in a reactive material before the main shock has arrived. It is to be expected that jet velocity may be raised above twice the particle velocity since droplets spalled from points around the upstream wall will collide along the central cavity-axis and travel forward with greater velocity to conserve momentum as in a shaped-charge jet. To account for the measured values of the jet velocity a two-dimensional simulation is needed.

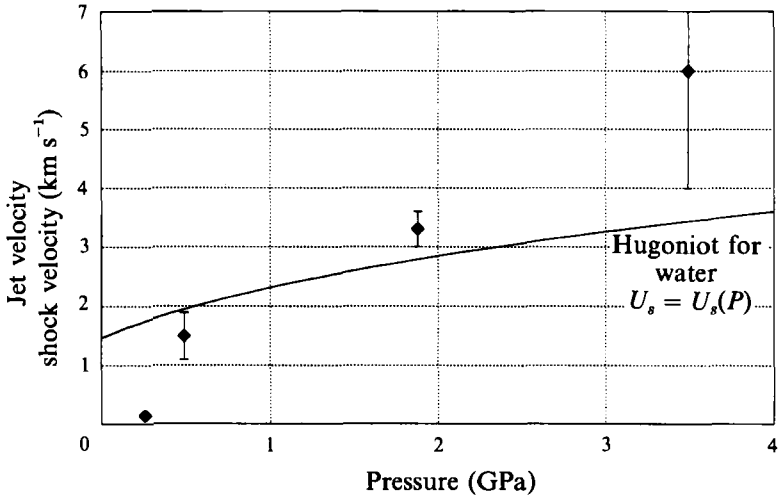

FIGURE 9. The variation of jet velocity with incident shock pressure for a 6 mm cavity. The Hugoniot for water divides the graph into two regions. In the lower region the jet velocity is less than the shock velocity and the shock crosses the cavity ahead of the jet. In the upper region the jet arrives at the downstream wall first and may send out a shock in the material downstream of the cavity ahead of the collapse shock.

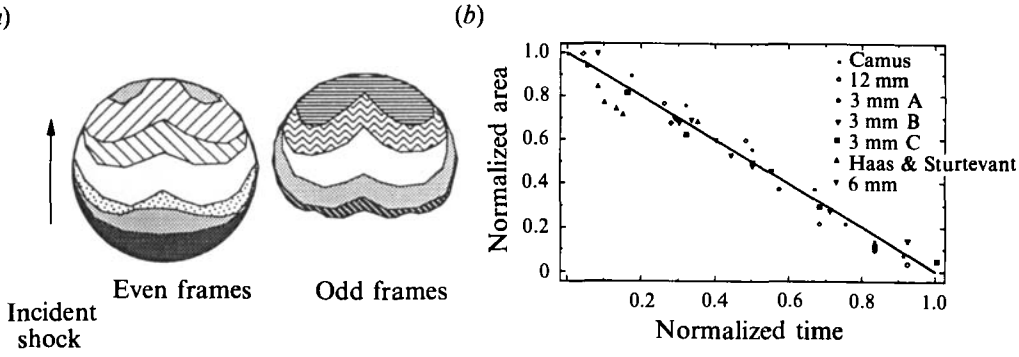

FIGURE 10. (*a*) Superimposed cavity wall shapes. (*b*) Various cylindrical collapses (including the present work) demonstrate that the area enclosed by the cavity as it collapses decreases linearly with time. All the collapses from the present work are at a pressure of 0.3 GPa. The coding A, B, C is described in the text.

Figure 10(*a*) shows successive superimposed cavity boundaries from the sequence of figure 3 and indicates how the upstream wall deforms and involutes as the shock passes over the cavity. The downstream wall retains its integrity up to the final stages of the collapse. The area enclosed by each successive cavity boundary normalized by the initial cavity area is plotted against time (normalized by the collapse time) in figure 10(*b*). The cavity collapse time is defined to be the time from the incident shock hitting the upstream wall to the time at which the liquid jet hits the downstream wall. Data for the collapse of other cylindrical cavities are displayed alongside those for figure 3: three different cavity sizes collapsed in gelatine are shown. The codings A, B and C refer to a void collapsing adjacent to a 3 mm solid particle embedded close to the cavity in the flow. Each of the letters represents a different orientation of the particle with respect to the cavity and the shock front. Two further sets of data taken from other work (Camus 1971: Haas & Sturtevant

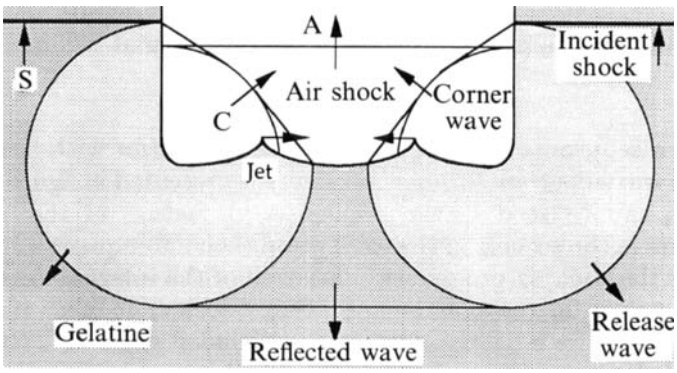

FIGURE 11. The interaction of a flat-walled cavity with a shock. Waves include the incident shock, S, the air shock, A, the corner waves, C and the release waves R.

1987) are presented. That of Camus is for the collapse of a 3 mm disc-shaped bubble of air in water whilst that of Haas & Sturtevant is for a 50 mm diameter cylinder of helium collapsing in air. The data suggest that the area of these cylindrical cavities (and hence their volume) decreases linearly with time. This result holds for each set of experimental data considered which is remarkable given the range of cavity dimensions and shock stimuli used. To our knowledge this particular feature of cavity collapse has not been treated theoretically.

Analysis of the position of the light flashes produced in figure 5 indicates that the bright flash, J, observed initially is positioned midway between those observed in frame (iii). The source of this initial luminescence is believed to be the violent shock-heating of a pocket of gas trapped between the jet and the far cavity wall at the moment before impact. The jet then impacts and as the lobes, L, are isolated and compressed the gas pockets begin to luminesce in frame (iii). The duration of temperatures sufficient to cause gas luminescence can be estimated to be about a microsecond. A sequence taken at similar framing rates has already been presented (figure 4). In this sequence a high-speed jet is seen crossing a 6 mm cavity ahead of the incident shock. A second cavity is obscured by the shock and is at the final stages of collapse in frame (iii) where light emission can be observed. In this sequence, one lobe is seen to persist longer than the other. This is believed to be due to an asymmetric collapse by the cavity due to an interaction between the cavities (Blake & Gibson 1987). This would result in the jet in the first cavity deviating towards that in the second, so isolating a lobe larger on the right side than the left. This larger volume of gas may explain the persistence of the luminescence on this side.

Sonoluminescence from cavities created by acoustic fields has been discussed by many authors (for a review see Young 1989). For water a continuum spectrum of wavelengths shifted to the blue has been observed. The spectral intensity distribution can be fitted to that of a black-body radiator with a colour temperature of 8800 K. Walton, in Dear *et al.* (1988), attributes the luminescence (observed in 3 mm collapsing cavities in gelatine using an image intensifier to time-average the light emission) to 'free-radical creation and radiative recombination'.

The creation of high temperatures within a collapsing cavity is a very complex and highly dynamic process. Results presented here suggest that the highest temperatures are created inside a cavity at the final moments of collapse and are associated with the impact of the jet and the later compression of an isolated pair of gas pockets. These lobes would be replaced by a toroidal pocket of gas in a three-

dimensional cavity. It should also be noted that hydrodynamic and viscous effects in the liquid may also be producing high temperatures that will not be observed as luminescence.

4.2. *Other collapse geometries*

In figure 6, two sequences showing the collapse of cavities with flat rear walls are presented. The wave diagram for such a collapse is presented in figure 11. Each of the labelled waves can be seen in the sequences. A feature of the collapses is the formation of jets in the corners of the cavity and their subsequent migration towards one another as the collapse progresses. Variation of the internal angle of the corner gives different values for the average migration velocity; 46 m s^{-1} for square-walled cavities and 33 m s^{-1} for a triangular cavity of included angle 67°. The jet formation can be regarded as a self-similar motion of the corner as the cavity closes. Engineering such cavity shapes in an explosive would allow several jet-impact, and thus initiation, sites from each inclusion as a shock wave ran through the matrix.

5. Conclusions

The present experiments have described a systematic investigation of jet formation in the asymmetric collapse of single cavities by shock waves of varying strengths. Such asymmetric collapses will also occur when the flow field around a cavity is perturbed by the presence of a solid boundary. An important criterion characterizing the closure was the collapse time. The collapse of a cylindrical cavity at low shock pressures proceeded by involution of the upstream wall into a constant-velocity jet which penetrated the stationary downstream wall to form a pair of counter-rotating linear vortices. These then travelled downstream in the flow behind the shock. Two lobes of compressed gas were isolated by the jet and the temperatures in these were sufficiently high that gas-luminescence was observed.

As cavity diameter was reduced or collapse-shock pressure increased, the velocity of the liquid jet increased. At elevated shock pressures, the jet velocity was not constant through the collapse and above a critical shock pressure the jet velocity exceeded the shock velocity in the surrounding liquid. After the jet hit the downstream wall a shock wave was transmitted which travelled ahead of the shock in the liquid. Also, the area enclosed inside the cylindrical cavity (and thus its volume) was found to decrease linearly with time as the collapse proceeded. This is an empirical result which could be usefully considered by theoreticians.

In rectangular geometries the flat upstream wall was found to develop jets which ran across the wall during collapse. These originated from the corners of the cavity with the migration velocity being higher for triangular cavities than for rectangular ones.

The work presented has shown cavities collapsing in isolation. The features of the collapse are changed markedly by the interaction of solid particles and surfaces close by. These interactions will be the subject of future papers.

N.K.B. thanks ICI for a CASE studentship and the Royal Commission for the Exhibition of 1851 for a research fellowship for the period over which this work was carried out. We thank Professor M. B. Lesser for several useful discussions during the course of the research.

REFERENCES

BENJAMIN, T. B. & ELLIS, A. T. 1966 The collapse of cavitation bubbles and the pressures thereby produced against solid boundaries. *Phil. Trans. R. Soc. Lond.* A **260**, 221–240.

BESANT, W. H. 1859 *Hydrostatics and Hydrodynamics*. Cambridge University Press.

BIRKHOFF, G., MACDOUGALL, D. P., PUGH, E. M. & TAYLOR, G. I. 1948 Explosives with lined cavities. *J. Appl. Phys.* **19**, 563–582.

BLAKE, J. R. & GIBSON, D. C. 1987 Cavitation bubbles near boundaries. *Ann. Rev. Fluid Mech.* **19**, 99–123.

BOURNE, N. K. 1989 Shock interactions with cavities. Ph.D. thesis, University of Cambridge.

BOURNE, N. K. & FIELD, J. E. 1989 Cavity collapse in a heterogeneous commercial explosive. In *Proc. Ninth Symp. (Intl) on Detonation, Portland, Oregon*, pp. 869–878. Office of Naval Research, Washington.

BOURNE, N. K. & FIELD, J. E. 1991 Bubble collapse and the initiation of explosion. *Proc. R. Soc. Lond.* A **435**, 423–435.

BOWDEN, F. P. & YOFFE, A. D. 1952 *Initiation and Growth of Explosion in Liquids and Solids*. Cambridge University Press.

BRUNTON, J. H. 1967 Erosion by liquid shock. In *Intl Conf. on Rain Erosion* (ed. A. A. Fyall & R. B. King), pp. 821–823. RAE, UK.

BRUNTON, J. H. & CAMUS, J.-J. 1970 The application of high-speed photography to analysis of flow in cavitation and drop-impact studies. *Proc. Intl Conf. on High Speed Photography* (ed. W. G. Hyzer & W. G. Chase), pp. 444–449. Soc. Motion Picture & Television Engrs, New York.

CAMUS, J.-J. 1971 High-speed flow in impact and its effect on solid surfaces. Ph.D. thesis, University of Cambridge.

CHAUDHRI, M. M., ALMGREN, L.-A. & PERSSON, A. 1982 High-speed photography of the interaction of shocks with voids in condensed media. *15th Intl Congr. on High-Speed Photography and Photonics, San Diego*, pp. 388–394. Soc. Photo Optical Instrumentation Engrs.

CHAUDHRI, M. M. & FIELD, J. E. 1974 The role of rapidly compressed gas pockets in the initiation of condensed explosives. *Proc. R. Soc. Lond.* A **340**, 113–128.

COLEY, G. D. & FIELD, J. E. 1973 The role of cavities in the initiation and growth of explosion in liquids. *Proc. R. Soc. Lond.* A **335**, 67–86.

COOK, S. S. 1928 Erosion by water hammer. *Proc. R. Soc. Lond.* A **260**, 221–240.

DEAR, J. P. 1985 The fluid mechanics of high-speed impact. Ph.D. thesis, University of Cambridge.

DEAR, J. P. & FIELD, J. E. 1988*a* A study of the collapse of arrays of cavities. *J. Fluid Mech.* **190**, 409–425.

DEAR, J. P. & FIELD, J. E. 1988*b* High-speed photography of surface geometry effects in liquid/solid impact. *J. Appl. Phys.* **63**, 1015–1021.

DEAR, J. P., FIELD, J. E. & WALTON, A. J. 1988 Gas compression and jet formation in cavities collapsed by a shock wave. *Nature* **332**, 505–508.

FIELD, J. E., LESSER, M. B. & DEAR, J. P. 1985 Studies of two-dimensional liquid wedge impact and their relevance to liquid-drop impact problems. *Proc. R. Soc. Lond.* A **401**, 225–249.

FREY, R. B. 1985 Cavity collapse in energetic materials. In *Eighth Symp. (Intl) on Detonation, Albuquerque, New Mexico, July*, pp. 68–80. Office of Naval Research, Washington.

GILMORE, F. R. 1952 The growth and collapse of a spherical bubble in a viscous compressible liquid. *Calif. Inst. of Tech. Hydrodyn. Lab. Rep.* 26–4.

GRANT, M. McD. & LUSH, P. A. 1987 Liquid impact on a bilinear elastic–plastic solid and its role in cavitation erosion. *J. Fluid Mech.* **176**, 237–252.

HAAS, J.-F. & STURTEVANT, B. 1987 Interaction of weak shock waves with cylindrical and spherical inhomogeneities. *J. Fluid Mech.* **181**, 41–76.

HUTCHINGS, I. M., ROCHESTER, M. C. & CAMUS, J.-J. 1977 A rectangular bore gas gun. *J. Phys* E: *Sci. Instrum.* **10**, 455–457

JOHNSON, J. N. 1987 Hot spot reaction under transient pressure conditions *Proc. R. Soc. Lond.* A **413**, 329–350.

KORNFELD, M. & SUVOROV, L. 1944 On the destructive action of cavitation. *J. Appl. Phys.* **15**, 495–506.

LAUTERBORN, W. & BOLLE, H. 1975 Experimental investigations of cavitation-bubble collapse in the neighbourhood of a solid boundary. *J. Fluid Mech.* **72**, 391–399.

LEIPER, G. A., KIRBY, I. J. & HACKETT, A. 1985 Determination of reaction rates in intermolecular explosives using the electromagnetic particle velocity gauge. In *Eighth Symp. (Intl) on Detonation, Albuquerque, New Mexico, July*, pp. 187–195. Office of Naval Research, Washington.

LEIPER, G. A. & STEELE, A. F. 1984 Design and calibration of a PMMA gap test. *ICI Rep.* NR321A.

MADER, C. L. 1964 The two-dimensional hydrodynamic hot-spot. *Los Alamos Natl Lab. Rep.* LA-3077, June.

MADER, C. L. & KERSHNER, J. D. 1985 The three dimensional hydrodynamic hot-spot model. In *Eighth Symp. (Intl) on Detonation, Albuquerque, New Mexico, July*, pp. 42–51. Office of Naval Research, Washington.

MARSH, S. P. 1980 *LASL Shock Hugoniot Data.* University of California Press.

MITCHELL, A. C. & NELLIS, W. J. 1982 Equation of state and electrical conductivity of water and ammonia shocked to the 100 GPa (1 Mbar) pressure range. *J. Chem. Phys.* **76**, 6273–6281.

PARSONS, C. A. & COOK, S. S. 1919 Investigations into the causes of corrosion or erosion of propellors. *Trans. Inst. Nav. Archit.* **61**, 223–277.

PLESSET, M. S. & CHAPMAN, R. B. 1971 Collapse of an initially spherical vapour cavity in the neighbourhood of a solid boundary. *J. Fluid Mech.* **47**, 283–290.

RAYLEIGH, LORD 1917 On the pressure developed during the collapse of a spherical cavity. *Phil. Mag.* **34**, 94–98.

STARKENBERG, J. 1981 Ignition of solid high explosive by the rapid compression of an adjacent gas layer. In *Seventh Symp. (Intl) on Detonation, Anapolis, Washington*, pp. 3–16. Office of Naval Research, Washington.

TAYLOR, P. A. 1985 The effects of material microstructure on the shock-sensitivity of porous granular explosives. In *Eighth Symp. (Intl) on Detonation, Albuquerque, New Mexico, July*, pp. 26–33. Office of Naval Research, Washington.

TOMITA, Y. & SHIMA, A. 1986 Mechanisms of impulsive pressure generation and damage pit formation by bubble collapse. *J. Fluid Mech.* **169**, 535–564.

TOMITA, Y., SHIMA, A. & OHNO, T. 1984 Collapse of multiple gas bubbles by a shock wave and induced impulsive pressures. *J. Appl. Phys.* **56**, 125–131.

VOGEL, A., LAUTERBORN, W. & TIMM, R. 1989 Optical and acoustic investigations of the dynamics of laser-produced cavitation bubbles near a solid boundary. *J. Fluid Mech.* **206**, 299–338.

WALSH, J. M. & RICE, M. H. 1957 Dynamic compression of liquids from measurements of strong shock waves. *J. Chem. Phys.* **26**, 815–830.

WALTERS, J. K. & DAVIDSON, J. F. 1962 The initial motion of a gas bubble formed in an inviscid liquid. Part 1. The two-dimensional bubble. *J. Fluid Mech.* **12**, 408–416.

WALTERS, J. K. & DAVIDSON, J. F. 1963 The initial motion of a gas bubble formed in an inviscid liquid. Part 2. The three-dimensional bubble and the toroidal bubble. *J. Fluid Mech.* **17**, 321–336.

YOUNG, F. R. 1989 *Cavitation.* McGraw-Hill.